Structural Basis of Inhibitor Affinity to Variants of Human Carbonic Anhydrase II[†,⊥]

Satish K. Nair,[‡] Joseph F. Krebs,[§,∥] David W. Christianson,*[,‡] and Carol A. Fierke*[,§]

Department of Chemistry, University of Pennsylvania, Philadelphia, Pennsylvania 19104-6323, and Department of Biochemistry, Duke University Medical Center, Box 3711, Durham, North Carolina 27710

Received October 26, 1994; Revised Manuscript Received January 3, 1995[⊗]

ABSTRACT: The activities and structures of certain L198 variants of human carbonic anhydrase II (CAII) have been reported recently [Krebs, J. F., Rana, F., Dluhy, R. A., & Fierke, C. A. (1993) *Biochemistry 32,* 4496−4505; Nair, S. K., & Christianson, D. W. (1993) *Biochemistry 32,* 4506−4514]. In order to understand the structural basis of enzyme−inhibitor affinity, we now report the dissociation rate and equilibrium constants for acetazolamide and dansylamide binding to 13 variants of CAII containing substituted amino acids at position 198. These data indicate that inhibitor affinity is modulated by the hydrophobicity and charge of the 198 side chain. Furthermore, we have determined crystal structures of L198R, L198E, and L198F CAIIs complexed with the transition state analog acetazolamide. The substituted benzyl side chain of L198F CAII does not occlude the substrate association pocket, and it is therefore not surprising that this substitution has minimal effects on catalytic properties and inhibitor binding. Nevertheless, the F198 side chain undergoes a significant conformational change in order to accommodate the binding of acetazolamide; the same behavior is observed for the engineered side chain of L198R CAII. In contrast, the engineered side chain of L198E CAII does not alter its conformation upon inhibitor binding. We conclude that the mobility and hydrophobicity of residue 198 side chains affect enzyme−inhibitor (and enzyme−substrate) affinity, and these structure−function relationships are important for understanding the behavior of carbonic anhydrase isozyme III, which bears a wild-type F198 side chain. Finally, these structures provide a foundation for modulating inhibitor affinity from the perspective of the enzyme rather than the inhibitor; this approach may be of use in the design of CAII-based zinc biosensors.

Carbonic anhydrase II (CAII)[1] is the most efficient of the seven known isozymes of carbonic anhydrase found in higher vertebrates (Tashian, 1989). In the human erythrocyte, CAII catalyzes the reversible hydration of carbon dioxide to bicarbonate ion and acid (H^+) with $k_{cat}/K_M = 1.5 \times 10^8\ M^{-1}\ s^{-1}$ [for recent reviews, see Coleman (1986), Lindskog (1986), Silverman and Lindskog (1988), and Christianson (1991)]. Although catalytic turnover is limited by the transfer of the product proton to extraneous buffer (Silverman & Tu, 1975; Jonsson et al., 1976), the measured turnover rate of $1 \times 10^6\ s^{-1}$ is nearly 300-fold greater than that of carbonic anhydrase III, the least efficient of the carbonic anhydrase isozymes (Tu et al., 1983). Moreover, CAII demonstrates a significantly greater susceptibility to inhibition by sulfonamides than isozyme III (Sanyal et al., 1982); for example, the transition state analog acetazolamide binds to wild-type CAII with $K_d = 0.09\ \mu M$ (this study) and to wild-type CAIII with $K_I = 40\ \mu M$ (LoGrasso et al., 1991).

The structure of CAII from human blood, determined and refined to 1.54 Å resolution (Hakånsson et al., 1992), reveals that the catalytically obligatory zinc ion resides at the base of a 15 Å deep cleft. Enzyme residues H94, H96, and H119 coordinate to zinc, and the catalytically active nucleophile, hydroxide ion (Coleman, 1967; Lindskog & Coleman, 1973), completes a tetrahedral metal coordination polyhedron. Important polar residues in the active site include T199, which accepts a hydrogen bond from zinc-bound hydroxide and donates a hydrogen bond to E106 (Eriksson et al., 1986, 1988; Hakånsson et al., 1992), and H64, which serves as a proton shuttle in the conversion of zinc-bound water into zinc-bound hydroxide (Steiner et al., 1975; Tu et al., 1989). A hydrophobic pocket adjacent to zinc-bound hydroxide has been proposed to constitute a precatalytic association site for substrate carbon dioxide (Lindskog, 1986), and this pocket is in fact the binding site of the only known competitive inhibitor for the CO_2 hydration reaction, phenol (Simonsson et al., 1982; Nair et al., 1994). The structural requirements for this pocket have been delineated in extensive genetic−structural studies of V143 at the base of the pocket (Fierke et al., 1991; Alexander et al., 1991) and V121 (Nair et al., 1991) and L198 (Krebs et al., 1993; Nair &

[†] We thank the NIH for Grants GM45614 (D.W.C.) and GM40602 (C.A.F) and the ONR for Grant ONR N00014-92-J-1851 (D.W.C.) in support of this work. S.K.N. is supported in part by NIH Training Grant GM07229. C.A.F. received an American Heart Association Established Investigator Award and a David and Lucille Packard Foundation Fellowship in Science and Engineering.

[⊥] Atomic coordinates of each final model have been deposited in the Brookhaven Protein Data Bank (Bernstein et al., 1977), with reference codes as follows: L198R CAII−AZA complex, 1YDD; L198E CAII−AZA complex, 1YDA; L198F CAII−AZA complex, 1YDB; L198F CAII, 1YDC.

* Authors to whom correspondence should be addressed.

[‡] University of Pennsylvania.

[§] Duke University Medical Center.

[∥] Current address: The Scripps Research Institute, 10666 N. Torrey Pines Rd., La Jolla, CA 92037.

[⊗] Abstract published in *Advance ACS Abstracts,* March 15, 1995.

[1] Abbreviations: CAII, carbonic anhydrase II; CAIII, carbonic anhydrase III; WT, wild type, L198R, leucine-198→arginine; L198E, leucine-198→glutamate; L198F, leucine-198→phenylalanine, etc., using the one-letter amino acid codes; AZA, acetazolamide; DNSA, dansylamide; Tris, tris(hydroxymethyl)aminomethane; EDTA, (ethylenedinitrilo)tetraacetic acid.

0006-2960/95/0434-3981$09.00/0

Christianson, 1993) at the mouth of the pocket. The so-called deep water molecule, which is displaced by phenol and therefore presumably displaced by substrate, resides at the mouth of this pocket (Eriksson, 1986, 1988; Hakånsson et al., 1992).

The three-dimensional structures of L198E and L198H CAIIs reveal that the substituted side chains of each variant pack against a flanking hydrophobic surface (Nair & Christianson, 1993), such that the hydrophobic→hydrophilic substitutions result in only 19-fold and 10-fold relative reductions, respectively, in CO_2 hydrase activity (Krebs et al., 1993). Although the structure of L198R CAII shows that the guanidinium side chain of R198 protrudes into the hydrophobic pocket, virtually occluding the precatalytic CO_2 association site, this variant exhibits only a 17-fold loss in CO_2 hydrase activity (Krebs et al., 1993; Nair & Christianson, 1993).

Here, the structural basis of residual catalytic activities in these CAII variants is illuminated by kinetic and structural studies of variant−transition state analog complexes. We now report the three-dimensional structures of L198R and L198E CAIIs complexed with the transition state analog acetazolamide (AZA) at 2.1 Å resolution. Additionally, the structures of inhibitor-free and inhibitor-bound forms of L198F CAII have been determined at resolutions of 1.95 and 1.9 Å, respectively. Our kinetic and structural studies of inhibitor binding allow us to further understand the role of residue 198 in modulating the activity of carbonic anhydrase isozymes II and III. Importantly, differences in CO_2 hydrase activity, the pK_a of zinc-bound solvent, and sulfonamide inhibitor affinity measured for these isozymes (LoGrasso et al., 1991; Lindskog et al., 1991; Ren et al., 1991; Sanyal et al., 1982; Eriksson & Liljas, 1993) are not solely due to variations at residue 198. Additionally, the structural study of CAII variant−inhibitor complexes allows us to develop a structure-based rationale for the improvement of enzyme−inhibitor affinity, not from the perspective of the inhibitor but instead from the perspective of the target enzyme. This novel approach may be useful in the optimization of CAII-based zinc biosensor designs (Thompson & Jones, 1993).

EXPERIMENTAL PROCEDURES

Protein Expression and Purification. CAII genes with mutations at L198 were prepared by site-directed mutagenesis and sequenced, and CAII was induced in BL21(DE3) pLysS cells containing pCAM-a1 encoding either wild-type or mutant CAII as described (Krebs et al., 1993). Cells were pelleted and a crude lysate was prepared by EDTA/lysozyme lysis, followed by the addition of $MgSO_4$ and DNase I (5 mM and 1 μg/mL final concentration, respectively). Cellular remnants were then removed by centrifugation (20000*g*, 20 min) (Krebs & Fierke, 1993). These lysates, containing 5−30 μM CAII, were filtered through a 0.2 μm filter and used directly for the determination of inhibitor binding. Leu-198 variants were purified from these cell extracts using sulfonamide affinity chromatography at pH 8.0 (Osborne & Tashian, 1975) followed by S-Sepharose ion exchange chromatography (Alexander et al., 1993). The concentration of CAII was determined either from stoichiometric titration of esterase activity using acetazolamide (Pocker & Stone, 1967) or from absorbance at 280 nm using a molar absorptivity of $5.4 \times 10^4\ M^{-1}\ cm^{-1}$ (Tu & Silverman, 1982).

Inhibitor Binding. Dansylamide (DNSA) dissociation constants were determined by measuring an increase in fluorescence (excitation = 280 nm, emission = 470 nm) upon binding DNSA to CAII (Chen & Kernohan, 1967) at 25 °C in 20 mM Tris−sulfate (pH 8.0), using concentrations of CAII (0.01−1.5 μM) 4−10-fold smaller than the observed K_d. The fluorescence signal was measured 1−5 min after the addition of DNSA. The dissociation constants determined for CAII in crude lysates were identical to those using purified CAII. Binding constants and error estimates (asymptotic standard error) were determined using the Kaleidagraph (Synergy Software) curve-fitting program with eq 1. Acetazolamide (AZA) binding was assayed by competition with bound DNSA as a decrease in fluorescence (excitation = 280 nm, emission = 470 nm) indicative of a decrease in the concentration of the E·DNSA complex. These titrations contained the following: CAII (10−70 nM), DNSA (5−20 μM), Tris−sulfate (20 mM, pH 8.0, 25 °C), and varied concentrations of AZA (0−5 mM). The AZA dissociation constant was calculated from these data using eq 2:

$$\text{fraction Fl} = (\text{Fl} - \text{IF})/(\text{EP} - \text{IF}) = \frac{1}{1 + K_{\text{DNSA}}/[\text{DNSA}]} \quad (1)$$

$$\text{fraction Fl} = (\text{Fl} - \text{EP})/(\text{IF} - \text{EP}) = \frac{1}{1 + (K_{\text{DNSA}}/[\text{DNSA}])(1 + [\text{AZA}]/K_{\text{AZA}})} \quad (2)$$

where Fl is the observed fluorescence, EP is the fluorescence end point, IF is the initial fluorescence, and K_{AZA} and K_{DNSA} are the dissociation constants for acetazolamide and dansylamide, respectively.

The rate constants for association of DNSA with CAII, k_{on}, and dissociation of DNSA, k_{off}, from CAII·DNSA complexes were determined using CAII in crude cell lysates. The formation of a CAII·DNSA complex was monitored by the time-dependent increase in fluorescence (excitation = 280 nm, emission using an output filter = 470 nm) after rapidly mixing DNSA (0.14−28 μM) with CAII in 20 mM Tris−SO_4 (pH 8.0, 25 °C), using a Kin-Tek stopped-flow spectrofluorimeter. The ratio of [DNSA]/[CAII] was ≥4, so that complex formation followed pseudo-first-order kinetics. A pseudo-first-order rate constant, k_{obs}, was calculated by fitting the time course to a single-exponential function:

$$\text{fraction Fl} = (\text{Fl} - \text{IF})/(\text{EP} - \text{IF}) = 1 - e^{-k_{obs}t} \quad (3)$$

where Fl is the fluorescence at a given time, EP is the fluorescence end point, and IF is the initial fluorescence. The rate constants for the association, k_{on}, and dissociation, k_{off}, of DNSA were determined from the slope and intercept, respectively, of a plot of k_{obs} versus [DNSA]. In some cases, the dissociation rate constant, k_{off}, was also determined by diluting the E·DNSA complex into high concentrations of acetazolamide (10−100 μM) and measuring the time-dependent decrease in fluorescence. These data are also described by a first-order exponential. Binding constants and error estimates (asymptotic standard error) were determined using the Kaleidagraph (Synergy Software) curve-fitting program. In all cases, the errors were ≤20% of k_{off} and k_{on}.

Crystallography. Enzyme crystallizations were performed as previously described (Nair & Christianson, 1993). Crys-

Table 1: Data Collection and Refinement Statistics for CAII Variant−AZA Complexes

	L198R−AZA	L198E−AZA	L198F−AZA	L198F
no. of crystals	1	1	1	1
no. of measured reflections	20609	17409	26968	19379
no. of unique reflections	11425	10682	16033	14137
maximum resolution (Å)	2.1	2.1	1.9	1.95
R_{merge}[a]	0.093	0.084	0.096	0.094
no. of water molecules in final cycle of refinement	101	79	87	86
no. of reflections used in refinement	9724	9179	14317	14065
completeness of data (%)	80	75	83	79
R factor[b]	0.187	0.181	0.167	0.165
rms deviation from ideal bond lengths (Å)	0.013	0.015	0.012	0.012
rms deviation from ideal bond angles (deg)	1.1	3.2	2.8	2.9
rms deviation from ideal dihedral angles (deg)	26.9	26.0	26.4	26.1
rms deviation from improper dihedral angles (deg)	1.36	1.33	1.19	1.15

[a] R_{merge} for replicate reflections: $R = \sum|I_{hi} - \langle I_h\rangle|/\sum\langle I_h\rangle$; I_{hi} is the intensity measured for reflection h in data set i, and $\langle I_h\rangle$ is the average intensity calculated for reflection h from replicate data. [b] Crystallographic R factor: $R = \sum||F_o| - |F_c||/\sum|F_o|$; $|F_o|$ and $|F_c|$ are the observed and calculated structure factors, respectively.

tals of CAII variant−AZA complexes were prepared by soaking pregrown crystals in a precipitant buffer solution containing 5 mM acetazolamide for up to 1 week. Suitable crystals of the CAII−dansylamide complex could not be prepared due to crystal cracking, nor was this particular complex amenable to cocrystallization. For X-ray data collection, crystals were mounted and sealed in 0.5 mm glass capillaries along with a small portion of the precipitant buffer. A Rigaku RU-200 rotating anode generator supplied Cu Kα radiation, and a Siemens X-100A multiwire area detector, equipped with Charles Supper double X-ray focusing mirrors, was used for data acquisition. The crystal-to-detector distance was set at 10 cm, and the detector swing angle was fixed between 20° and 25° in at least three runs per experiment. Data frames of 0.1° oscillation about ω were collected, with exposure times of 60 s/frame. Raw data frames were analyzed for intensities in reciprocal space, and these intensities were corrected for Lorentz and polarization effects using the BUDDHA package (Durbin et al., 1986). Replicate and symmetry-related structure factors derived from these intensities were scaled and merged using PROTEIN (Steigemann, 1974). Crystals of CAII variants and their acetazolamide complexes were isomorphous with the wild-type enzyme (Alexander et al., 1991) and belonged to space group $P2_1$, with typical unit cell parameters of a = 42.7 Å, b = 41.7 Å, c = 73.0 Å, and β = 104.6°. Relevant data collection and reduction statistics are recorded in Table 1.

The refined structure of wild-type CAII (Alexander et al., 1991), less the atoms of L198 and active site solvent molecules, served as the starting point of each refinement. The atomic coordinates of L198R and L198E CAIIs complexed with AZA were refined against the observed data using PROLSQ (Hendrickson, 1985). The simulated annealing protocol of Brünger (1987) installed on a Silicon Graphics IRIS workstation was employed for the refinement of both L198F CAII and its complex with AZA. All model building was done with the graphics software FRODO (Jones, 1985) installed on an Evans and Sutherland PS390 interfaced with a VAXstation 3500. In the refinement of each structure, the variant side chain of residue 198, active site solvent molecules, and acetazolamide were built into difference electron density maps (calculated with structure factors and phases derived from the in-progress atomic model) when the crystallographic R factor dropped below 0.20. During the course of refinement, solvent molecules were routinely examined and deleted if their thermal B factors exceeded 50 Å^2. For each structure, refinement converged smoothly to a final R factor within the range 0.165−0.187. Each final model has excellent stereochemistry with rms deviations from ideal bond lengths and angles within the ranges of 0.012−0.015 Å and 1.1−3.2°, respectively. Pertinent refinement statistics are recorded in Table 1.

RESULTS

Inhibitor Binding. To investigate the role of the L198 side chain in the avidity and specificity of sulfonamide binding to CAII, a variety of single amino acid variants at position 198 were constructed (Krebs et al., 1993), and the dissociation constants for two inhibitors, dansylamide (DNSA) and acetazolamide (AZA), were determined. The dissociation constants for DNSA binding to CAII variants were measured as the increase in fluorescence at 470 nm due to fluorescence energy transfer between CAII tryptophans and DNSA (Chen & Kernohan, 1967) (Figure 1A, Table 2). The dissociation constants for AZA (Figure 1B, Table 2) were measured by competition with dansylamide as the decrease in fluorescence due to the disappearance of E·DNSA and the concomitant formation of an E·AZA complex. In all cases, the data are well described by a single observed dissociation constant (eqs 1 and 2). Sulfonamide binding to wild-type CAII is pH independent from 7 to 9; binding decreases at both high and low pH, reflecting the ionization of the sulfonamide moiety ($pK_a \approx 9$) and the zinc-bound water molecule ($pK_a \approx 7$; Kernohan, 1966; Lindskog & Thorslund, 1968). The pK_a of the zinc−water increases (≥0.5 pH unit) for the L198R, L198H, and L198K CAII variants (Krebs et al., 1993; Krebs, 1992), which alters the pH dependence of sulfonamide binding; the values listed in parentheses in Table 2 are corrected for this difference.

Amino acid substitutions at position 198 affect the binding of AZA and DNSA in a strikingly different manner. For DNSA, binding is decreased only by the substitution of a negatively charged amino acid (L198E) at this position; all other substitutions have either no effect or increase binding up to 12-fold. In fact, a comparison of the K_{DNSA} values for wild-type and L198A CAII indicates that the L198 side chain destabilizes the E·DNSA complex by 1.5 kcal/mol at 25 °C.[2] This result is consistent with modeling studies by Vedani

[2] $\Delta\Delta G = -2.303RT \log(K_d^{mutant}/K_d^{WT})$.

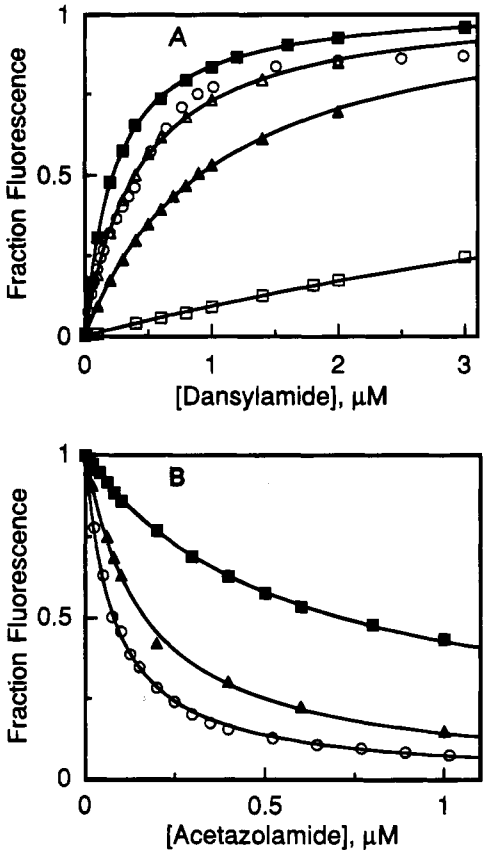

FIGURE 1: Determination of DNSA and AZA dissociation constants in 20 mM Tris−sulfate (pH 8.0, 25 °C). (A) Small aliquots (1−5 μL) of DNSA were added to 1 mL of 0.05 μM CAII variants [L198R in crude lysate (■), L198F in crude lysate (△), pure L198F (○), wild type in crude lysate (▲), and L198E in crude lysate (□)], and the increase in fluorescence (excitation = 280 nm, emission = 470 nm) was assayed. The K_{DNSA} values (listed in Table 2) were determined by fitting the data to eq 1 using the curve-fitting program Kaleidagraph. (B) CAII variants were preincubated with DNSA [0.025 μM L198R in crude lysate with 4 μM DNSA (■), 0.02 μM wild-type in crude lysate with 15 μM DNSA (▲), and 0.05 μM pure L198F with 5 μM DNSA (○)], such that ≥90% of the enzyme formed a CAII·DNSA complex. Then, small aliquots (1−5 μL) of AZA were added to 1 mL of the enzyme mixture, and the decrease in fluorescence (excitation = 280 nm, emission = 470 nm) was monitored. The K_{AZA} values (Table 2) were determined by fitting the data to eq 2 using the K_{DNSA} values measured in (A).

and Meyer (1984) suggesting that the L198 side chain makes unfavorable steric interactions with ortho-substituted benzenesulfonamides. Similarly, amino acid substitutions at T200 and C206 enhance DNSA binding (Krebs & Fierke, 1993), suggesting that this protein loop may form unfavorable steric contacts with DNSA. These data clearly indicate that DNSA does not optimally fit into the active site of CAII, and therefore, tighter binding can be achieved by changing the structure of the active site cavity.

However, many amino acid substitutions at position 198 increase the K_d for the tighter binding inhibitor, AZA (Table 2). In this case, comparison of the K_{AZA} of L198A to that of wild type indicates that the leucine side chain provides 1 kcal/mol of favorable interaction energy with AZA. Furthermore, with the exception of positively charged amino acids (arginine and lysine) and valine, the dissociation constants for AZA (but not DNSA) are related to the hydrophobicity of the substituted side chain at position 198. The linear correlation of $-\log K_{AZA}$ versus the transfer free energy of amino acids between either cyclohexane and water

Table 2: Equilibrium and Rate Constants for Sulfonamide Inhibitors Binding to L198 Variants of CAII[a]

variant	K_{AZA}[b] (nM)	K_{DNSA}[b] (μM)	k_{off}/k_{on}[c] (μM)	k_{on}[c] ($\mu M^{-1}\ s^{-1}$)	k_{off}[c] (s^{-1})
wild type	9.6 (8.8)[d]	0.93 (0.86)[d]	1.3	0.29	0.38
L198W	8.6 (7.6)	0.32 (0.28)	0.46	0.070	0.036
L198F	5.8 (5.4)	0.39 (0.36)	0.30	0.90	0.27
L198M	14 (14)	0.1[e] (0.1)	0.19	0.58	0.11
L198V	100 (96)	0.46 (0.44)	0.69	0.11	0.78
L198C	15 (14)	1.1 (1.0)	1.4	0.33	0.46
L198A	60 (53)	0.08 (0.07)	0.11	0.97	0.11
L198H	330 (180)	1.2 (0.67)	0.86	0.25	0.21
L198G	67 (57)	1.0 (0.85)	1.3	0.64	0.86
L198S	340 (320)	0.23 (0.22)	0.38	0.053	0.020
L198E	280[f]	9.3[f]	11.3	0.006	0.071
L198K	22 (18)	0.46 (0.37)	0.75	0.092	0.069
L198R	86 (66)	0.24 (0.18)	0.12	0.092	0.011

[a] Determined in 20 mM Tris−SO_4 (pH 8.0, 25 °C). [b] The K_{AZA} and K_{DNSA} values were measured as described in the legend of Figure 1. The errors were ≤10% of the dissociation constant. [c] The dissociation (k_{off}) and association (k_{on}) rate constants were determined as described in the legend of Figure 3. The errors were ≤20% of the rate constants. [d] The dissociation constants, corrected for the pK_a of the zinc−water in each variant (Krebs et al., 1993; Krebs, 1992; Ren et al., 1991) by $(K_d)_{corr} = (K_d)_{obs}/(1 + 10^{(pK_a - pH)})$, are shown in parentheses. [e] Taken from Krebs and Fierke (1993). [f] pH dependence of catalysis is bell shaped (Krebs et al., 1993).

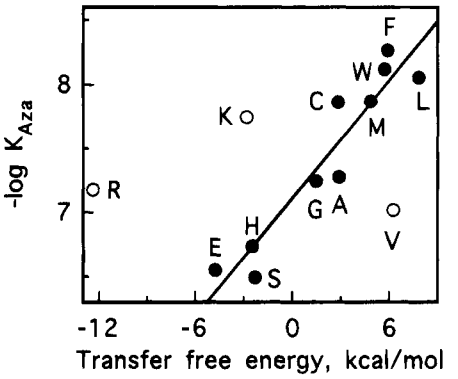

FIGURE 2: Plot of $-\log K_{AZA}$ for binding of AZA to CAII variants with amino acid substitutions at position 198 versus hydrophobicity of the substituted amino acid, as measured by the corrected free energy of transfer of amino acid side chain analogs from cyclohexane to water (Radzicka & Wolfenden, 1988; Sharp et al., 1991). The symbols indicate the substituted amino acid using the one-letter amino acid codes. The data (excluding the open symbols) are fit to a line using the fitting program Kaleidagraph.

(Figure 2) or octanol and water [corrected for size as in Sharp et al. (1991); Radzicka & Wolfenden, 1988; Fauchère & Pliska, 1983] yields slopes of 0.15 (R = 0.95) and 0.25 (R = 0.85). These results indicate that the hydrophobic nature of the side chain at position 198 modulates the avidity of AZA binding, as well as the catalytic activity of CAII (Krebs et al., 1993). Interestingly, K_{AZA} for the L198F variant is tighter than that for wild type and falls on the line in the hydrophobicity plot (Figure 2). However, substitution of a positively charged amino acid at position 198 creates variants that bind sulfonamide better than predicted by their hydrophobicity. This effect is probably due to a favorable electrostatic interaction between the positive charge introduced on the enzyme and the deprotonated sulfonamide anion inhibitor bound to the enzyme (RSO_2NH^-) (Kanamori & Roberts, 1983).

Kinetics of DNSA Binding. During the course of determining K_{DNSA}, we observed that several amino acid substitu-

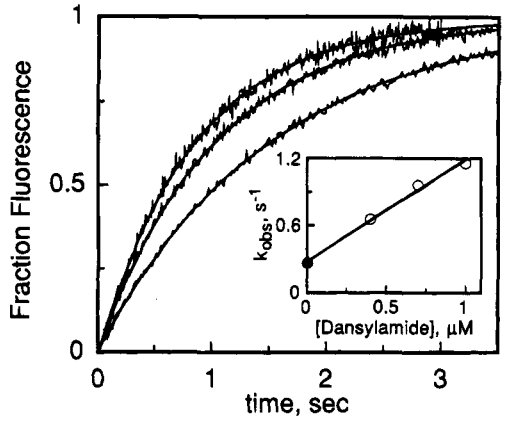

FIGURE 3: Measurement of the association and dissociation rate constants for DNSA binding to L198F CAII in 20 mM Tris−sulfate (pH 8.0, 25 °C). Purified L198F CAII was mixed rapidly with 3.5 vol of DNSA in a Kin-Tek stopped-flow spectrofluorimeter to give a final concentration of 0.1 μM CAII with either 0.4, 0.7, or 1.0 μM DNSA. The fluorescence at 470 nm, indicative of the formation of an E·DNSA complex, was measured as a function of time, and the data are fit by a single-exponential decay (eq 3). The inset shows the concentration dependence of the observed rate constant for binding DNSA, where the association and dissociation rate constants can be estimated from the slope = 0.90 ± 0.05 μM^{-1} s^{-1} and intercept = 0.27 ± 0.03 s^{-1}, respectively. The rate constant at zero DNSA was determined from the observed first-order exponential decay of fluorescence when 0.35 μM L198F CAII plus 1.5 μM DNSA (forming E·DNSA) was diluted 3.5-fold into 7 μM AZA, which rapidly binds E (formed by dissociation of DNSA) to make E·AZA.

tions at position 198 significantly diminish the rate of formation of the E·DNSA complex. Therefore, we measured the kinetics of DNSA binding (Figure 3, Table 2). The rate of formation was monitored by increased fluorescence energy transfer between the enzyme and DNSA. Under pseudo-first-order conditions ([DNSA]/[CAII] ≥4), the appearance of the binary complex is described by a single first-order exponential (eq 3), which is dependent on the concentration of DNSA (Figure 3). For a simple association reaction, the observed rate constant under pseudo-first-order conditions may be approximated by $k_{obs} = k_{on}$[DNSA] + k_{off}, where k_{on} and k_{off} are the association and dissociation rate constants, respectively (Fierke & Hammes, 1994). In a linear plot of k_{obs} versus [DNSA] (Figure 3, inset), the slope is k_{on} and the intercept is k_{off} (listed in Table 2). The fact that the ratio of the rate constants (k_{off}/k_{on}) is consistent with the measured K_{DNSA} indicates that the assumption of a simple association reaction is reasonable. However, the association rate constants that are slower than diffusion-controlled (10^7−10^8 M^{-1} s^{-1}) may suggest a more complicated mechanism.

These data indicate that substitutions at position 198 have significant effects on both the association and dissociation rate constants. Small aliphatic residues (A, G, C), as well as larger aromatic residues that pack in such a manner as to form a wider mouth to the pocket (F, H) (this work; Nair & Christianson, 1993), increase the association rate constant modestly (up to 3-fold). Substitution of bulky side chains (W) or hydrophilic residues (R, K, E, S) decreases k_{on} significantly (up to 50-fold). This decreased k_{on} may suggest that larger side chains sterically impede the association of DNSA, e.g., as indicated by the movement of the arginine side chain in the L198R CAII·AZA complex (described in the next section). Conversely, the dissociation rate constant for DNSA from the CAII·DNSA complex is decreased for all but three substitutions, and decreases in k_{off} up to 30-fold are observed for the insertion of bulky or hydrophilic residues at position 198. Again, conformational changes of the substituted side chain may decrease the dissociation rate constant of the bound sulfonamide inhibitor.

L198R CAII−Acetazolamide Complex. The difference electron density map of the L198R CAII−acetazolamide complex in Figure 4 reveals that the side chain of R198 undergoes a significant conformational change upon inhibitor binding. In native L198R CAII, the variant guanidinium side chain protrudes into the active site cavity and partially blocks the hydrophobic pocket (Nair & Christianson, 1993). However, the side chain of R198 rotates significantly about side chain torsion angles χ_1, χ_3, and χ_4 in order to accommodate the inhibitor molecule (Table 3, Figure 5), and these bond rotations result in a less favorable conformation (Bhat et al., 1979) for the side chain. Additionally, these conformational changes place the guanidinium group of R198 near a hydrophobic patch defined by enzyme residues P202, F131, L141, and L204. However, R198 is not nested as deeply in this patch as the variant side chains of L198E and L198H CAIIs (Nair & Christianson, 1993); moreover, the guanidinium group of R198 only makes van der Waals contacts with P202 and F131 and no hydrogen bonds with active site residues or ordered solvent molecules. Interestingly, while electron density for the bifurcated guanidinium side chain of R198 is weak in the variant enzyme—perhaps indicative of some mobility (Nair & Christianson, 1993)—this residue

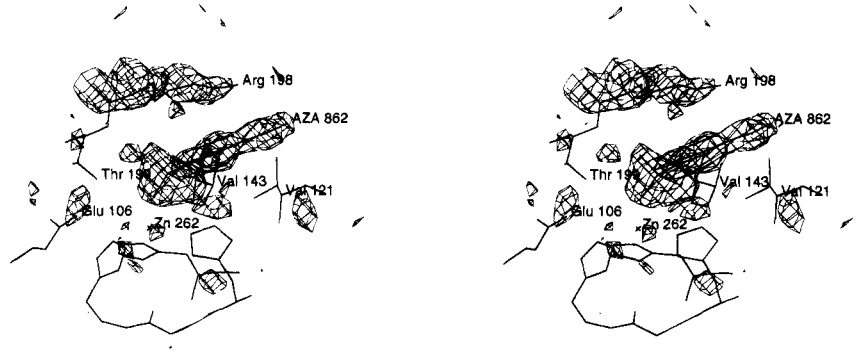

FIGURE 4: Difference electron density map of the L198R CAII−acetazolamide complex, calculated with Fourier coefficients ($|F_o| - |F_c|$) and phases calculated from the final model less the atoms of R198 and acetazolamide and active site solvent molecules. Refined atomic coordinates are superimposed on the map (contoured at 2.5σ); E106, V121, V143, R198, T199, acetazolamide, and zinc are indicated. The side chain of R198 rotates significantly about side chain torsion angles χ_1, χ_3, and χ_4 in order to accommodate the inhibitor molecule, and these bond rotations result in a less favorable conformation for the side chain.

Table 3: Comparison of Residue 198 Torsion Angles (Degrees) in CAII Variants and Their AZA Complexes

wild type	CAII[a]	CAII·AZA[b]	L198R CAII[c]	L198R·AZA	L198E CAII[c]	L198E·AZA	L198F CAII	L198F·AZA
ϕ	−73	−70	−73	−65	−66	−65	−65	−65
ψ	+155	+149	+156	+149	+156	+149	+150	+148
χ_1	−71	−64	−67	−19	−72	−66	−54	−79
χ_2	+179	+180	−179	−170	+152	+174	+13	+152
χ_3			+101	+118	−18	−26		
χ_4			−68	−141				

[a] Alexander et al., 1991. [b] Vidgren et al., 1990. [c] Nair & Christianson, 1993.

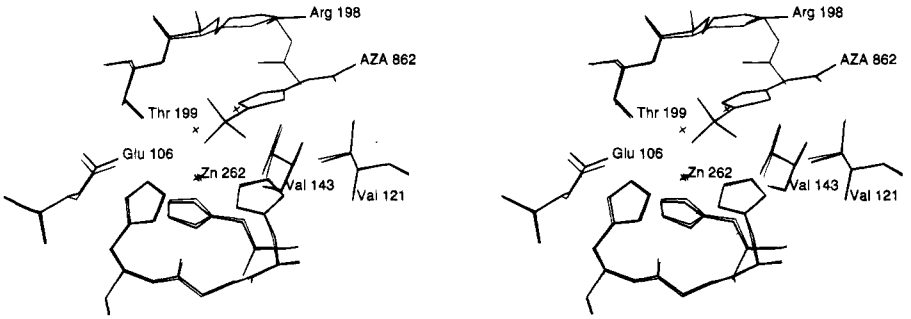

FIGURE 5: Superposition of L198R CAII (thin lines) and its complex with acetazolamide (thick lines). Enzyme residues E106, V121, V143, R198, and T199, acetazolamide, and the active site zinc are indicated. The side chain of R198 undergoes a significant conformational change in order to accommodate binding of the inhibitor molecule.

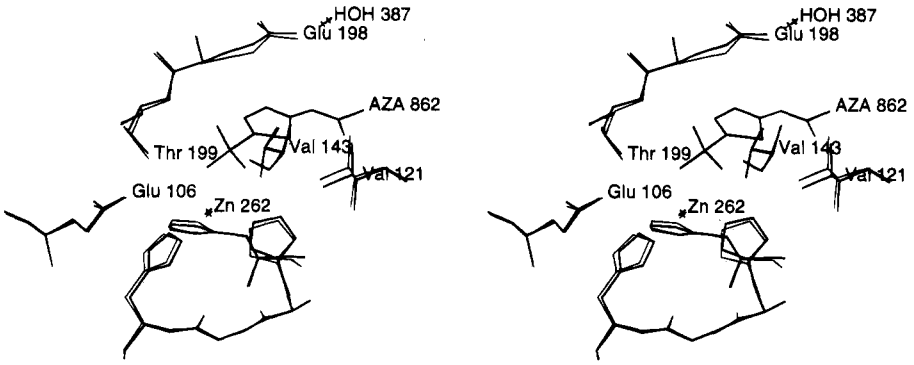

FIGURE 6: Superposition of L198E CAII (thin lines) and its complex with acetazolamide (thick lines). Enzyme residues E106, V121, V143, E198, and T199, acetazolamide, and the active site zinc are indicated. Since the side chain of E198 does not "cap" the hydrophobic pocket of the enzyme active site, its movement is not required to accommodate inhibitor binding.

is more clearly defined in the electron density map of the enzyme−inhibitor complex (Figure 4).

Significantly, a conformational change for H64, the catalytic proton shuttle (Steiner et al., 1975; Tu et al., 1989), is also triggered by acetazolamide binding to L198R CAII: the imidazole side chain undergoes a rotation of 96° about side chain torsion angle χ_1 to the "out" conformation observed in certain CAII structures (Baldwin et al., 1989; Krebs et al., 1991; Nair & Christianson, 1991; Prugh et al., 1991; Alexander et al., 1993; Jain et al., 1994; Smith et al., 1994). Although such a rotation is typically observed in structures of CAII complexes with inhibitors requiring such movement for binding (Baldwin et al., 1989), there are no such steric requirements for acetazolamide binding. Moreover, no rotation for H64 is observed upon the binding of acetazolamide by native blood CAII (Eriksson et al., 1986, 1988), nor is a H64 rotation observed in any other acetazolamide complexes of L198 variants of CAII.

There are no other significant changes between the structure of the L198R CAII−acetazolamide complex and the inhibitor-free variants, and the rms deviation of Cα atoms between the two structures is 0.18 Å. Overall, the refined structure of the L198R CAII−acetazolamide complex is also similar to that of the wild-type enzyme, and the rms deviation of Cα atoms between the L198R CAII·AZA complex and wild-type CAII is 0.17 Å.

L198E CAII−Acetazolamide Complex. No significant conformational changes are triggered in the L198E CAII active site upon acetazolamide binding (Table 3). Thus, the polar side chain of E198 remains packed against the flanking hydrophobic surface defined by active site residues P202, F131, L141, and L204 (Nair & Christianson, 1993). Since the E198 side chain does not "cap" the hydrophobic pocket of the enzyme active site (e.g., like R198), its movement is not required to accommodate inhibitor binding. The closest contact between the E198 side chain and the inhibitor is a van der Waals interaction between E198 Oε1 and the thiadiazole nitrogen of acetazolamide. A least-squares superposition of the native L198E CAII−acetazolamide complex and the inhibitor-free variant reveals that the two structures are essentially identical (Figure 6); the rms deviation of Cα atoms between the two structures is 0.19 Å. Similarly, there are no significant structural changes in the L198E CAII−acetazolamide complex relative to the wild-type enzyme; the rms deviation in Cα atoms between the two structures is 0.22 Å.

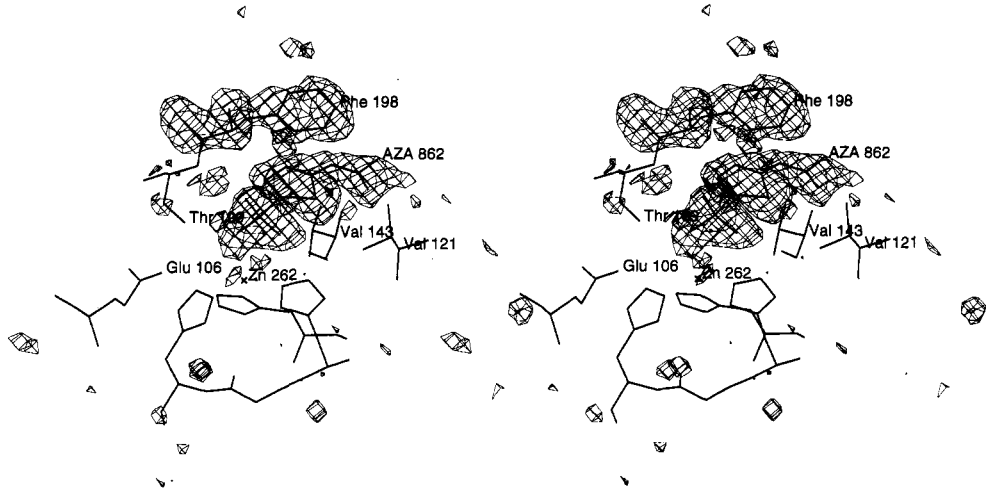

FIGURE 7: Difference electron density map of the L198F−acetazolamide complex, calculated with Fourier coefficients ($|F_o| - |F_c|$) and phases calculated from the final model less the atoms of F198 and acetazolamide and active site solvent molecules. The map is contoured at 2.5σ, and refined atomic coordinates are superimposed; E106, V121, V143, F198, T199, acetazolamide, and zinc are indicated. The heteroatomic thiadiazole ring of acetazolamide interacts with the aromatic benzyl ring of F198 in an edge-to-face orientation.

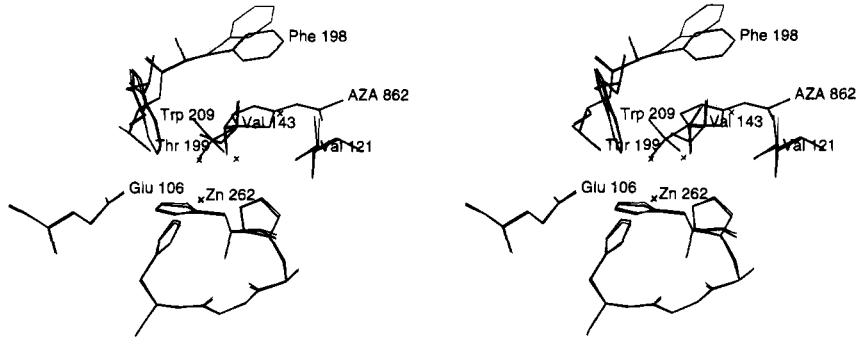

FIGURE 8: Superposition of L198F CAII (thin lines) and its complex with acetazolamide (thick lines). Enzyme residues E106, V121, V143, F198, T199, and W209 and the active site zinc are indicated. The phenyl side chain of F198 undergoes significant conformational changes about torsion angles χ_1 and χ_2 in order to accommodate inhibitor binding.

L198F CAII and Its Acetazolamide Complex. The benzyl side chain of F198 packs against the hydrophobic wall defined by flanking residues P202, F131, L141, and L204. The conformation of the F198 side chain therefore is quite similar to that of the side chains of E198 and H198 (Nair & Christianson, 1993; Table 3). In contrast with the conformation of F198 in the hydrophobic pocket of wild-type CAIII (Eriksson & Liljas, 1993), which constricts the mouth of the pocket, the L198F substitution in CAII widens the mouth of the hydrophobic pocket. For reference, the closest contact between F198 and zinc-bound hydroxide in L198F CAII is 5.3 Å, whereas this distance is decreased to 4.6 Å in CAIII.

The torsion angles of F198 are reported in Table 3. As in L198E and L198H CAIIs, torsion angle χ_2 appears to deviate from optimal values (Ponder & Richards, 1987) in order to optimize contact surface area between the side chain and its flanking hydrophobic region. A superposition of wild-type and L198F CAIIs results in an rms deviation in Cα atoms of 0.17 Å between the two structures.

The three-dimensional structure of L198F CAII complexed with acetazolamide reveals that the phenyl side chain of F198 undergoes significant conformational changes about torsion angles χ_1 and χ_2 in order to accommodate inhibitor binding (a difference electron density map is found in Figure 7, and side chain torsion angles are reported in Table 3). The heteroaromatic thiadiazole ring of acetazolamide interacts with the aromatic benzyl ring of F198 in an edge-to-face orientation (Burley & Petsko, 1988). Even so, F198 endures conformational changes that maintain an unfavorable torsion angle χ_2 (Ponder & Richards, 1987). However, despite these conformational changes, acetazolamide binds to L198F CAII both more rapidly and more tightly than it does to the wild-type enzyme (Table 2). Overall, the structure of L198F CAII does not undergo any significant conformational changes upon binding the inhibitor: the rms deviation in Cα atoms superimposed on the inhibitor-free structure is 0.12 Å (a superposition of L198F CAII and its complex with acetazolamide is found in Figure 8).

DISCUSSION

Structural Role of Residue 198 in Carbonic Anhydrase Isozymes. Residue L198 is not strictly conserved among the carbonic anhydrase isozymes, and isozyme III contains F198 (Lloyd, 1986). The bulky phenyl group of F198 in CAIII is postulated to account for reduced CO_2 hydrase activity, the depressed pK_a of zinc-bound solvent, and the diminished affinity for sulfonamide inhibitors (Eriksson & Liljas, 1993). Unlike F198 in the L198F variant of CAII, the refined crystal structure of CAIII reveals that the side chain of F198 protrudes into the hydrophobic pocket of CAIII and contacts zinc-bound hydroxide (Eriksson & Liljas, 1993). Indeed, replacement of the phenyl group by a smaller aliphatic side chain in F198L CAIII results in a variant that exhibits an increased k_{cat}/K_M and an elevation in the pK_a of the zinc-bound water molecule by 1 unit (LoGrasso et al., 1991). However, it should be noted that several other residues in

the CAIII active site also contribute to activity differences between CAII and CAIII (LoGrasso et al., 1991; Chen et al., 1993). Just as a successful CAII→CAIII conversion requires more than changes only at F198, a successful CAIII→CAII conversion requires more than changes only at L198; Lindskog and colleagues demonstrate that L198F CAII exhibits catalytic activity and a zinc-bound solvent pK_a comparable to those of wild-type CAII (Lindskog et al., 1991; Ren et al., 1991).

Catalytic and binding constants for L198F CAII (Lindskog et al., 1991; Ren et al., 1991; this work), interpreted in light of its three-dimensional structure, suggest why this substitution alone is insufficient to convert CAII into CAIII. A principal difference is the fact that F198 in L198F CAII adopts a conformation different from the wild-type F198 side chain in CAIII. Additionally, since the bound conformation of AZA in complex with L198F CAII is similar to its bound conformation in complex with native blood CAII (Vidgren et al., 1990), and since the K_{AZA} is actually smaller for the L198F CAII·AZA complex, inhibitor binding is not compromised by the L198F substitution in CAII. Therefore, the structural basis for the differences in catalytic activity and inhibitor binding between CAII and CAIII is not represented by L198F CAII. The difference in the side chain conformation of F198 in the two isozymes may be mediated by other amino acid substitutions in bovine CAIII, including L141I and L204E (Tashian et al., 1980; Eriksson & Liljas, 1993), in the flanking hydrophobic wall.

Interestingly, attempts to occlude the hydrophobic pocket by the substitution of large side chains other than phenylalanine at position 198 in CAII have a substantial, but not severe, effect on catalytic activity (Krebs et al., 1993) and inhibitor binding (this work). Although the structure of L198R CAII reveals that the arginine side chain "caps" the hydrophobic pocket (Nair & Christianson, 1993), the structure of the L198R CAII·AZA complex reveals that the guanidinium side chain of R198 undergoes a conformational change to accommodate inhibitor binding. Similar conformational mobility of R198 probably accommodates CO_2 binding, thereby accounting for the significant residual catalytic activity observed in this variant (Krebs et al., 1993). Furthermore, deviations of $-\log K_{AZA}$ and $\log k_{cat}/K_M$ for L198R and L198K from the lines in structure−reactivity plots (Figure 2; Krebs et al., 1993) suggest that the positive charge on the side chain stabilizes both the negatively charged inhibitor and the transition state for CO_2 hydration by more than 1 kcal/mol.

The carboxylate oxygens of E198 do not form any hydrogen bonds with the inhibitor molecule. We note that the L198E substitution destabilizes the binding of sulfonamide inhibitors to this CAII variant, which is probably due to destabilization of the negatively charged inhibitor by the negative charges of E198. Interestingly, while dansylamide binding is lowered only by a factor of 10, binding of acetazolamide is lowered by nearly a factor of 30. We note that Oϵ2 of E198 is only 5.3 Å away from the terminal carboxylate oxygen of acetazolamide. Since this oxygen is present only in acetazolamide and not in dansylamide, this charge repulsion may account for the lower affinity of AZA for L198E CAII.

Design of a CAII-Based Zinc Biosensor. Thompson and Jones (1993) report the design of a fluorescence-based zinc biosensor that exploits the recognition and selectivity of zinc by apocarbonic anhydrase II (Coleman, 1965; Lindskog & Nyman, 1964). Briefly, a sulfonamide-based probe (dansylamide), which exhibits an enhancement of its fluorescence emission upon binding to zinc (Chen & Kernohan, 1967), is used to detect specific recognition of zinc by CAII when the zinc enzyme−inhibitor complex is formed (Thompson & Jones, 1993). In order to improve the signal-to-noise ratio of fluorescence emission by the enzyme−zinc−inhibitor ternary complex relative to that of the free inhibitor and apoenzyme, it is desirable to improve the affinity of the inhibitor for the enzyme active site.

Although the design for improved affinity may be approached by the structure-based design of tighter binding inhibitors (Bunn et al., 1994; Boriack et al., 1994), problems inherent in the stability of the inhibitor, the required spectral signature of the inhibitor, and the extraneous shifts in fluorescence by the inhibitor limit this approach (Thompson & Jones, 1993). Here, an alternate pathway for the design of tighter enzyme−inhibitor complexes are presented: instead of modifying the inhibitor structure to improve enzyme−inhibitor affinity, the enzyme structure is modified to improve enzyme−inhibitor affinity (Table 2). The unexpected short- and long-range structural changes accommodating AZA binding in its complexes with L198R CAII and L198F CAII demonstrate that high-resolution crystal structures of variant enzyme−inhibitor complexes reveal many of the features that modulate enzyme−inhibitor affinity; the data reported in Table 2 reveal that enzyme−inhibitor affinity can be enhanced by as much as 12-fold in the case of DNSA binding to L198A CAII. Combination of this side chain deletion with other substitutions that enhance DNSA binding, such as C206R or C206Y (K_{DNSA} = 0.02 μM; Krebs & Fierke, 1993), will likely lead to variants that bind DNSA as well as, or better than, wild-type CAII binds acetazolamide.

SUMMARY AND CONCLUSIONS

The hydrophobic pocket of CAII is critical for substrate association and inhibitor binding. Moreover, both the acetazolamide affinity and catalytic activity of CAII (Krebs et al., 1993) reflect the hydrophobicity and charge of the side chain at position 198. Replacement of L198 by larger residues, such as phenylalanine, in CAII has a minimal effect on catalysis and inhibitor binding due to preferential side chain packing and side chain conformational changes, resulting in a wider hydrophobic pocket. Although the substituted guanidinium side chain of L198R CAII appears to block the hydrophobic pocket, R198 is sufficiently mobile to accommodate sulfonamide inhibitors and, by inference, the substrate as it approaches the nucleophilic zinc-bound hydroxide. In contrast, the bulky benzyl side chain of F198 in CAIII occludes the hydrophobic pocket, possibly diminishing catalytic turnover and inhibitor affinity.

ACKNOWLEDGMENT

We thank Gang Hu and Steven Paterno for technical assistance in preparing and analyzing L198F CAII.

REFERENCES

Alexander, R. S., Nair, S. K., & Christianson, D. W. (1991) *Biochemistry 30*, 11064−11072.

Alexander, R. S., Kiefer, L. L., Fierke, C. A., & Christianson, D. W. (1993) *Biochemistry 32*, 1510−1518.
Baldwin, J. J., Ponticello, G. S., Anderson, P. S., Christy, M. E., Murcko, M. A., Randall, W. C., Schwam, H., Sugrue, M. F., Springer, J. P., Grove, J., Mallorga, P., Viader, M.-P., McKeever, B. M., & Navia, M. A. (1989) *J. Med. Chem. 32*, 2510−2513.
Bernstein, F. C., Koetzle, T. F., Williams, G. J. B., Meyer, E. F., Brice, M. D., Rodgers, J. R., Kennard, O., Shimanouchi, T., & Tasumi, M. (1977) *J. Mol. Biol. 112*, 535−542.
Bhat, T. N., Sasisekharan, V., & Vijayan, M. (1979) *Int. J. Pept. Protein Res. 13*, 170−184.
Boriack, P. A., Wood, J. K., Christianson, D. W., & Whitesides, G. M. (1994) *J. Med. Chem.* (submitted for publication).
Brünger, A. T. (1987) *XPLOR Manual*, Yale University Press, New Haven, CT.
Bunn, A. M. C., Alexander, R. S., & Christianson, D. W. (1994) *J. Am. Chem. Soc. 116*, 5063−5068.
Burley, S. K., & Petsko, G. A. (1988) *Adv. Protein Chem. 39*, 125−189.
Chen, R. F., & Kernohan, J. C. (1967) *J. Biol. Chem. 242*, 5813−5823.
Chen, X., Tu, C.-K., LoGrasso, P., Laipis, P. J., & Silverman, D. N. (1993) *Biochemistry 32*, 7861−7865.
Christianson, D. W. (1991) *Adv. Protein Chem. 42*, 281−355.
Coleman, J. E. (1965) *Biochemistry 4*, 2644−2655.
Coleman, J. E. (1967) *J. Biol. Chem. 242*, 5215−5219.
Coleman, J. E. (1986) in *Zinc Enzymes* (Bertini, I., Luchinat, C., Maret, W., & Zeppezauer, M., Eds.) pp 49−58, Birkhauser, Boston.
Durbin, R. M., Burns, R., Moulai, J., Metcalf, P., Freymann, D., Blum, M., Anderson, J. E., Harrison, S. C., & Wiley, D. C. (1986) *Science 232*, 1127−1132.
Eriksson, A. E., & Liljas, A. (1993) *Proteins: Struct., Funct., Genet. 16*, 29−42.
Eriksson, A. E., Jones, T. A., & Liljas, A. (1986) in *Zinc Enzymes* (Bertini, I., Luchinat, C., Maret, W., & Zeppezauer, M., Eds.) pp 317−328, Birkhauser, Boston.
Eriksson, A. E., Jones, T. A., & Liljas, A. (1988) *Proteins: Struct., Funct., Genet. 4*, 274−282.
Fauchère, J. L., & Pliska, V. (1983) *Eur. J. Med. Chem.−Chim. Ther. 18*, 369−375.
Fierke, C. A., & Hammes, G. G. (1994) Methods Enzymol. (in press).
Fierke, C. A., Calderone, T. L., & Krebs, J. F. (1991) *Biochemistry 30*, 11054−11063.
Hakånsson, K., Carlsson, M., Svensson, L. A., & Liljas, A (1992) *J. Mol. Biol. 227*, 1192−1204.
Hendrickson, W. A. (1985) *Methods Enzymol. 115*, 252−270.
Jain, A., Whitesides, G. M., Alexander, R. S., & Christianson, D. W. (1994) *J. Med. Chem. 37*, 2100−2105.
Jones, T. A. (1985) *Methods Enzymol. 115*, 157−171.
Jonsson, B.-H., Steiner, H., & Lindskog, S. (1976) *FEBS Lett. 64*, 310−314.
Kanamori, K., & Roberts, J. D. (1983) *Biochemistry 22*, 2658−2664.
Kernohan, J. C. (1966) *Biochim. Biophys. Acta 118*, 405−412.
Krebs, J. F. (1992) Investigation of the Roles of Hydrophobic Residues in Human Carbonic Anhydrase II Using Mutagenesis and Kinetic Analysis, Ph.D. Dissertation, Duke University, Durham, NC.
Krebs, J. F., & Fierke, C. A. (1993) *J. Biol. Chem. 268*, 948−954.
Krebs, J. F., Fierke, C. A., Alexander, R. S., & Christianson, D. W. (1991) *Biochemistry 30*, 9153−9160.
Krebs, J. F., Rana, F., Dluhy, R. A., & Fierke, C. A. (1993) *Biochemistry 32*, 4496−4505.
Lindskog, S. (1986) in *Zinc Enzymes* (Bertini, I., Luchinat, C., Maret, W., & Zeppezauer, M., Eds.) pp 307−316, Birkhauser, Boston.
Lindskog, S., & Nyman, P.-O. (1964) *Biochim. Biophys. Acta 85*, 462−474.
Lindskog, S., & Thorslund, A. (1968) *Eur. J. Biochem. 3*, 453−460.
Lindskog, S., & Coleman, J. E. (1973) *Proc. Natl. Acad. Sci. U.S.A. 70*, 2505−2508.
Lindskog, S., Behravan, G., Engstrand, C., Forsman, C., Jonsson, B.-H., Liang, Z., Ren, X., & Xue, Y. (1991) in *Carbonic Anhydrase* (Botre, F., Gros, G., & Storey, B. T., Eds.) pp 1−13, VCH, Weinheim, Germany.
Lloyd, J., McMillan, S., Hopkinson, D., & Edwards, Y. H. (1986) *Gene 41*, 233−239.
LoGrasso, P. V., Tu, C.-K., Jewell, D. A., Wynns, G. C., Laipis, P. J., & Silverman, D. N. (1991) *Biochemistry 30*, 8463−8470.
Nair, S. K., & Christianson, D. W. (1991) *J. Am. Chem. Soc. 113*, 9455−9458.
Nair, S. K., & Christianson, D. W. (1993) *Biochemistry 32*, 4506−4514.
Nair, S. K., Ludwig, P. A., & Christianson, D. W. (1994) *J. Am. Chem. Soc. 116*, 3659−3660.
Osborne, W. R. A., & Tashian, R. E. (1975) *Anal. Biochem. 64*, 297−303.
Pocker, Y., & Stone, J. T. (1967) *Biochemistry 6*, 668−678.
Ponder, J. W., & Richards, F. M. (1987) *J. Mol. Biol. 193*, 775−791.
Prugh, J. D., Hartman, G. D., Mallorga, P. J., McKeever, B. M., Michelson, S. R., Murcko, M. A., Schwam, H., Smith, R. L., Sondey, J. M., Springer, J. P., & Sugrue, M. F. (1991) *J. Med. Chem. 34*, 1805−1818.
Radzicka, A., & Wolfenden, R. (1988) *Biochemistry 27*, 1664−1670.
Ren, X. L., Jonsson, B. H., & Lindskog, S. (1991) *Eur. J. Biochem. 201*, 417−420.
Sanyal, G., Swenson, E. R., Pessah, N. I., & Maren, T. H. (1982) *Mol. Pharmacol. 22*, 211−220.
Sharp, K. A., Nicholls, A., Friedman, R., & Honig, B. (1991) *Biochemistry 20*, 9686−9697.
Silverman, D. N., & Tu, C.-K. (1975) *J. Am. Chem. Soc. 97*, 2263−2269.
Silverman, D. N., & Lindskog, S. (1988) *Acc. Chem. Res. 21*, 30−36.
Simonsson, I., Jonsson, B.-H., & Lindskog, S. (1982) *Biochem. Biophys. Res. Commun. 108*, 1406−1412.
Smith, G. M., Alexander, R. S., Christianson, D. W., McKeever, B. M., Ponticello, G. S., Springer, J. S., Randall, W. C., Baldwin, J. J., & Habecker, C. N. (1994) *Protein Sci. 3*, 118−125.
Steigemann, W. (1974) Ph.D. Thesis, Max-Planck-Institut für Biochemie, 8033 Martinsried bei München, Germany.
Steiner, H., Jonsson, B.-H., & Lindskog, S. (1975) *Eur. J. Biochem. 59*, 253−259.
Tashian, R. E. (1989) *BioEssays 10*, 186−192.
Tashian, R. E., Hewett-Emmett, D., Stroup, S. K., Goodman, M., & Yu, Y.-S. L. (1980) in *Biophysics and Physiology of Carbon Dioxide* (Bauer, C., Gros, G., & Bartels, H., Eds.) pp 165−176, Springer-Verlag, Berlin.
Thompson, R. B., & Jones, E. R. (1993) *Anal. Chem. 65*, 730−734.
Tu, C.-K., & Silverman, D. N. (1982) *Biochemistry 21*, 6353−6360.
Tu, C.-K., Sanyal, G., Wynns, G. C., & Silverman, D. N. (1983) *J. Biol. Chem. 258*, 8867−8871.
Tu, C.-K., Silverman, D. N., Forsman, C., Jonsson, B.-H., & Lindskog, S. (1989) *Biochemistry 28*, 7913−7918.
Vedani, A., & Meyer, E. F., Jr. (1984) *J. Pharm. Sci. 73*, 352−358.
Vidgren, J., Liljas, A., & Walker, N. P. C. (1990) *Int. J. Biol. Macromol. 12*, 342−344.

BI942504D